Desalination and Water Treatment
www.deswater.com
doi: 10.5004/dwt.2023.29480

290 (2023) 147–161
April

Polyethyleneimine modified spent coffee grounds as a novel bio-adsorbent for selective adsorption of anionic Congo red and cationic Methylene blue

Shuaishuai Wang, Wansheng Li, Guangfen Li*

State Key Laboratory of Separation Membranes and Membrane Processes, School of Materials Science and Engineering, Tiangong University, Tianjin, 300387, China, Tel.: +86 22 83955074; email: liguangfen@tiangong.edu.cn (G. Li), Tel.: +86 15075955972; email: 2583478201@qq.com (S. Wang), Tel.: +86 13821761586; 2318608512@qq.com (W. Li)

Received 24 October 2022; Accepted 13 March 2023

ABSTRACT

Here, a new renewable bio-adsorbent (SCG-PEI) was prepared by grafting polyethyleneimine (PEI) onto spent coffee grounds (SCG) surface. Effects of molecular weight and dosage of PEI, initial dye concentration, contact time, temperature and pH on the adsorption properties of SCG-PEI adsorbent for Congo red (CR) were comprehensively researched. The SCG-PEI adsorbent possesses higher adsorption capacity towards CR when using PEI with higher molecular weight. Adsorption capacity of SCG-PEI to CR (1,313 mg/g) is better than Methylene blue (MB, 814 mg/g) owing to the high content of amino groups in SCG-PEI adsorbent that has a selective adsorption to CR. The specific surface area of SCG-PEI sample is 18.336 m^2/g, and the pore volume is 0.0169 cm^3/g. Kinetic and isothermal analysis explored that the adsorption behavior of CR dye complies with Elovich kinetic model and Freundlich adsorption isotherm model. The adsorption mechanism further reveals that electrostatic force and pore filling are prominent effects for the higher adsorption of CR. The study provides an approach for preparing environmentally friendly and efficient adsorbents.

Keywords: Adsorption; Congo red; Methylene blue; Polyethyleneimine; Spent coffee grounds

1. Introduction

Currently, large quantities of wastewater disposed from textile, leather, paper-making industries contain organic dyes, heavy metals and other pollutants, which have posed a huge threat to the ecological environment. The occurrences of organic dyes in water bodies even in minor quantities have harmful impact on aquatic life because they possess non-biodegradable aromatic rings, decrease water transparency and hinder photosynthesis process [1]. Various methods for removal of dye pollutants are photocatalytic [2], biological [3], chemical (ions exchange [4]), physical (membrane separation [5]), and adsorption [6]). Among all these available techniques, adsorption is regarded as one of the most effective, fastest and simplest approach that leads to a promising application prospect.

Biomass resources such as argan nutshell [7], tea leaves [8], pericarp [9], ground nut shell [10] and coffee grounds [11] are abundant high-quality materials for the preparation of organic adsorbents, which creates solely possibility for final biodegradation. Spent coffee grounds (SCG) are flotsam of coffee beans to make coffee and are suitable for being used as adsorbents for various pollutants because of plenty pores present in their surface and interface. It also contains a lot of cellulose, hemicellulose, lignin and other organic substances making it chemically modified by different routes [12]. Recent studies show that the SCG related adsorbents can be basically divided into three categories:(i) pristine SCG [13]; (ii) activated carbons [14]; (iii) chemically modified SCG. Despite pristine SCG is capable of separating some pollutants from the sewage water, the removal ratio is still far from satisfactory. Activated carbons originated

* Corresponding author.

from SCG show higher specific surface and accessibility of surface functionality as it being used as adsorbents for purification of wastewater [15]. While, the preparation process of activated carbon is rather complex and energy consuming, which actually limits its further applications. Chemical modification of SCG has attracted many attentions because it introduces various functional groups by reacting with different types of materials on SCG surface [16] and provides opportunities to interact with other dye molecules. The multiple interaction forces between adsorbents and dyes are essential to an improvement in adsorption performance. Surfactant is the most common material used for chemical modification, which is cheap and environmentally friendly [17]. It is public knowledge that polyethyleneimine (PEI) contains plenty of nitrogenous function groups like –NH and $–NH_2$ groups, which can selectively bind with heavy metal ions and anionic dyes, and is an ideal surface modifier. In recent years, many researchers have combined PEI with various adsorbent materials to remove pollutions, and have achieved good results (starch nanocrystals [18], coffee waste [19], corncob [20], spent tea leaves [21]). All these researches proved that PEI is a novel candidate for functionalizing bio-adsorbents for the purpose of pollutants adsorption, and the attachment of PEI to the adsorbents provides a possibility for selectively building up the interaction with a specific sorbent. Up to date, there are few reports about using PEI modified coffee grounds adsorbent to adsorb dyes. The effects of intrinsic parameters and experimental parameters (molecular weight, dosage of PEI, initial concentration and pH of dye solution) on adsorption capacity and mechanism are unrevealed and their application in the purification of the sewage water is necessary to be strengthened.

In this study, different molecular weights and dosage of PEI were selected for the chemically modification of SCG. The surface morphology, chemical composition, degradation behavior and pore structure of PEI-SCG were comprehensively characterized. The influencing factors such as contact time, initial dye concentration, temperature, and pH on adsorption performance were explored. In addition, kinetic and isothermal studies on dye adsorption process were performed and the adsorption mechanism of anionic dye by SCG-PEI adsorbents was revealed.

2. Materials and methods

2.1. Materials

The original material of spent coffee grounds (SCG) was obtained from a local coffee shop in Tianjin, China. Methylene blue (MB) (M_w = 319.85 Da) and Congo red (CR) (M_w = 696.68 Da) were bought from Tianjin Institute of Fine Chemical Industry (Tianjin, China). Sodium hydroxide (NaOH) was purchased from Tianjin Fengchuan Chemical Reagent Technology Co., Ltd., (Tianjin, China). Polyethyleneimine (PEI) was provided by Shanghai Aladdin Biochemical Technology Co., Ltd., (Shanghai, China).

2.2. Preparation of SCG-PEI

SCG was washed with deionized water repeatedly until the filtrate was clear and transparent. After that it was dried in an oven at 60°C. To remove the oil content from the surface of SCG, dried SCG (1 g) and NaOH (25 mL, 0.1 M) solution were mixed and stirred in a 60°C water bath for 20 min. After the mixture was aspirated, the filtrate was poured out and the product was repeatedly washed until its pH was 8–9. After that, different molecular weights of PEI (same mass of SCG) were mixed to the SCG and stirred in a water bath for 1 h (23°C). Repeatedly washed the sample with distilled water until its pH was approximately equivalent to 7. Finally, the samples were dried for 5 h at 60°C, then grinded and sieved in powder form (250–300 μm). PEI with different molecular weights (600, 1800, 10,000 and 70,000) was utilized to yield a series of SCG samples, named as SCG-PEI-M_x, while, x changes from 1 to 4. The sample prepared without PEI was used as the control group, which was called SCG_0.

2.3. Characterization of adsorbents

The surface morphology of SCG_0 and SCG-PEI-M_x was photographed by scanning electron microscope (SEM, Hitachi H7650, Japan). The specific surface area and pore volume of SCG_0 and SCG-PEI-M_4 were tested (T = 300 K, P/P_0 = 0–1) by an automatic physical chemisorption instrument (BET, Autos orb-IQ-C, Quanta chrome, USA). The chemical composition of SCG_0 and SCG-PEI-M_x was determined by using Fourier-transform infrared spectroscopy (FTIR, Nicolai iS50, USA) in a range of 500–4,000 cm^{-1}. The thermal stability of SCG_0 and SCG-PEI-M_x between 25°C and 800°C (10°C/min), N_2 environment) was analyzed by thermogravimetric analyzer (TG, STA409F3, Hitachi, Japan). Elements (C, N, O) in SCG_0 and SCG-PEI-M_x were characterized by X-ray photoelectron spectrometer (XPS, Thermos Fisher Science, USA).

2.4. Adsorption experiments

CR and MB solutions with a concentration of 300 mg/L were prepared and then diluted to the desired concentration (100, 200 and 250 mg/L). Each sample (5 mg) was added to the dye solutions (30 mL) until reaching the adsorption equilibrium. The solution before and after dye adsorption was filtered by using a polytetrafluoroethylene needle filter having a pore size of 450 nm and then evaluated by UV-Vis's spectrophotometer (PerkinElmer Ultraviolet-35, USA). Eqs. (1)–(3) were used to calculate the adsorption capacity and removal rate of the adsorbents [22]. All concentration values were measured three times and averaged.

$$Q_e = \frac{\left(C_0 - C_e\right) \times V}{w} \tag{1}$$

$$Q_t = \frac{\left(C_0 - C_t\right) \times V}{w} \tag{2}$$

$$R = \frac{\left(C_0 - C_e\right)}{C_0} \times 100\% \tag{3}$$

where Q_e (mg/g) is the equilibrium adsorption capacity of adsorbents. Q_t (mg/g) is the adsorption capacity at time

t. R (%) is the removal rate of CR and MB. V (L) represents the volume of dye solutions. w (g) is the mass of the adsorbent. C_0 (mg/L) is the initial concentration of CR and MB. C_t (mg/L) and C_e (mg/L) represent the concentrations of dye solutions at time t and adsorption equilibrium.

Effects of contact time (0.5–72 h), temperature (298–328 K), pH (4–10), and original dye concentrations (100–300 mg/L) on the removal of CR and MB by SCG-PEI-M_4 were studied.

2.5. Adsorption isothermal and kinetics models

For studying the adsorption behavior of SCG-PEI-M_4 on CR in relation to the contact time, pseudo-first-order kinetic model [Eq. (4)], pseudo-second-order kinetic model [Eq. (5)] [23] and Elovich model [Eq. (6)] [24] were used to fit the adsorption behavior, respectively.

$$\ln\left(Q_e - Q_t\right) = \ln Q_e - k_1 t \tag{4}$$

$$\frac{t}{Q_t} = \frac{1}{k_2 Q_e^2} + \frac{t}{Q_e} \tag{5}$$

$$Q_t = \frac{1}{\beta}\ln\alpha\beta + \frac{1}{\beta}\ln t \tag{6}$$

where t (h) is the adsorption time. Q_e (mg/g) represents the equilibrium adsorption capacity. Q_t (mg/g) is the adsorption capacity at t time. k_1 (h^{-1}) and k_2 (g/mg·h) are the rate constants of the pseudo-first-order and pseudo-second-order kinetic models, respectively. α specifies the initial adsorption rate (mg/g·h). β represents the extent of surface coverage and the activation energy involved in chemisorption (g/mg).

Langmuir, Freundlich and Dubinin–Radushkevich (D-R) isothermal adsorption models were used to study the isothermal adsorption process of SCG-PEI-M_4, as shown in Eq. (7) [25], Eq. (8) [26] and Eqs. (9) and (10), respectively:

$$\frac{C_e}{Q_e} = \frac{1}{K_L Q_m} + \frac{C_e}{Q_m} \tag{7}$$

$$\ln Q_e = \ln K_F + \frac{1}{n}\ln C_e \tag{8}$$

$$\ln Q_e = \ln Q_m - K_{\mathrm{DR}}\,\epsilon^2 \tag{9}$$

$$\epsilon = RT\ln\left(1 + \frac{1}{C_e}\right) \tag{10}$$

where K_L (L/mg) and K_F [(mg/g)(L/mg)$^{1/n}$] represent the constants of Langmuir and Freundlich models, respectively. Q_e (mg/g) is the equilibrium adsorption capacity of adsorbent. Q_m (mg/g) represents the maximum adsorption capacity. $1/n$ means intensity parameter. C_e (mg/L) represents the equilibrium concentration of CR. K_{DR} (mol^2/J^2) is the D-R isotherm constant and ϵ specifies the Polanyi potential. R (8.314 J/mol·K) is the ideal gas constant.

2.6. Adsorption thermodynamics

For studying the Gibbs free energy change and effects of the basic thermodynamic parameters on the dye adsorption performance, Gibbs free energy change (ΔG), enthalpy change (ΔH) and entropy change (ΔS) were calculated, as follows [26]:

$$\Delta G = -RT\ln K \tag{11}$$

$$\Delta G = \Delta H - T\Delta S \tag{12}$$

$$\ln K = -\frac{\Delta H}{RT} + \frac{\Delta S}{R} \tag{13}$$

where K is the equilibrium constant, that is, Q_e/C_e. R (8.314 J/mol·K) is the ideal gas constant. T (K) is the experimental temperature; ΔG (kJ/mol) is the Gibbs free energy change; ΔH (kJ/mol) is the enthalpy change; ΔS (J/mol·K) is the entropy change.

3. Results and discussion

3.1. Characterizations of SCG_0 and SCG-PEI-M_x

3.1.1. SEM analysis

The surface morphologies of SCG_0 and SCG-PEI-M_x samples were imaged through SEM and displayed in

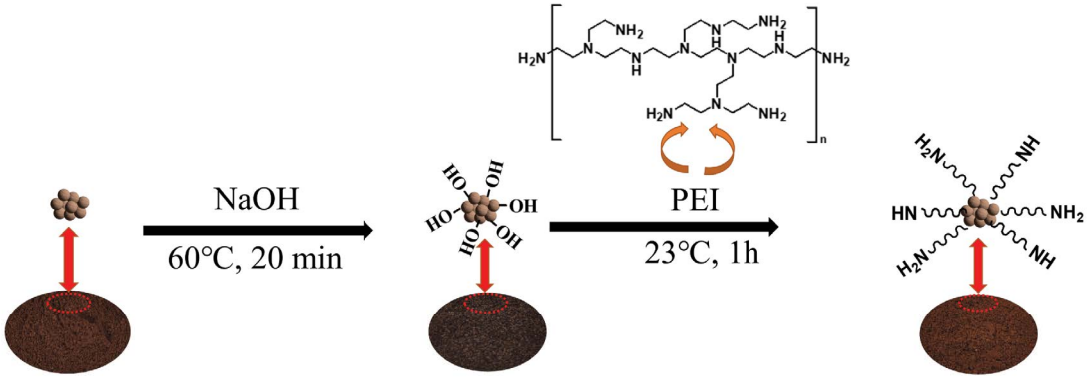

Fig. 1. Schematic preparation of SCG-PEI-M_x adsorbents.

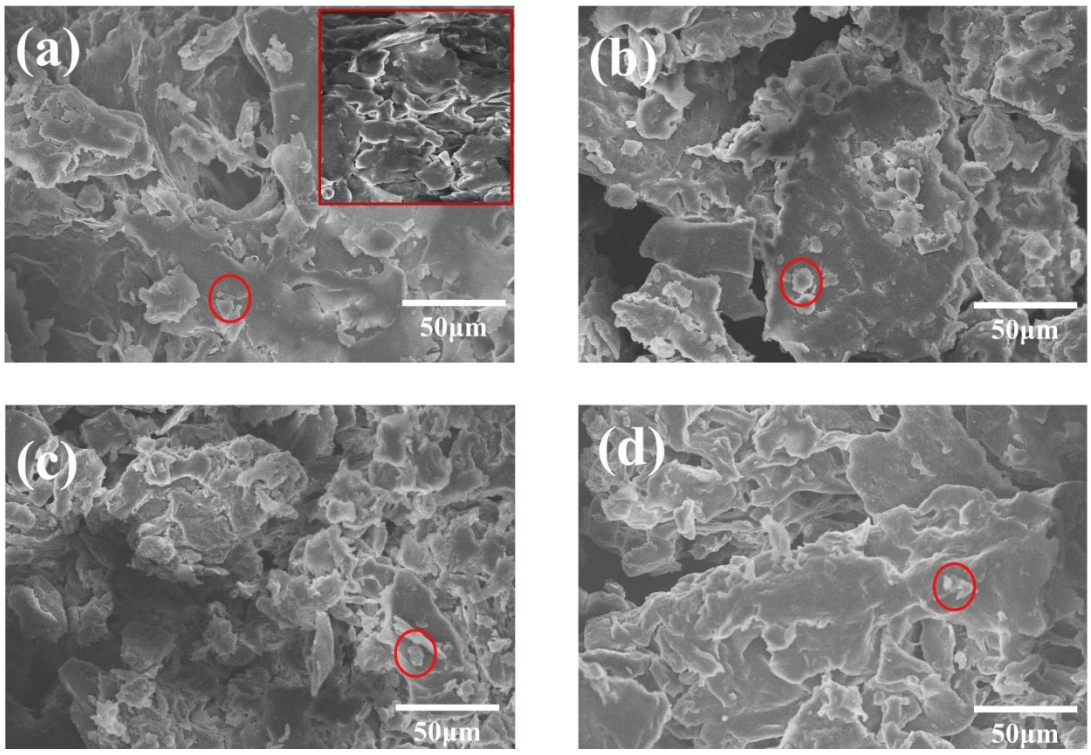

Fig. 2. Scanning electron microscopy images of SCG_0 (inset of a) and SCG-PEI-M_1, SCG-PEI-M_2, SCG-PEI-M_3, SCG-PEI-M_4 (a–d).

Fig. 2. Some irregular pore structures show on the surface of all samples, which are typical features of SCG (inset of Fig. 2a). This indicates that the adsorbents can have a certain adsorption effect by capturing pollutants molecules through pore filling. Compared to SCG_0 sample, the surface of all SCG-PEI-M_x samples appears rather rough and grainy due to the presence of PEI molecules (red circles in Fig. 2). And with the increase of molecular weight of PEI, the particle size on the sample surface becomes much bigger (Fig. 2a–c). This phenomenon becomes more pronounce in SCG-PEI-M_4 (Fig. 2d). The long PEI molecule chains are prone to entangle on SCG sample surface and thus create more active sites for adsorbing dyes. Therefore, using PEI with molecular weight of 70,000 to dope spent coffee grounds is more beneficial to obtain adsorbents with excellent capacity.

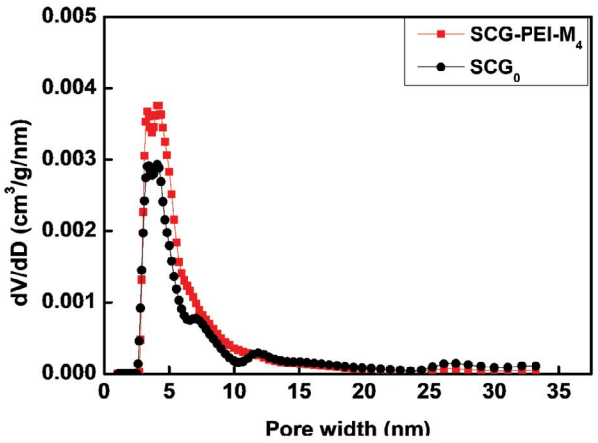

Fig. 3. Pore width distribution of SCG_0 and SCG-PEI-M_4.

3.1.2. BET analysis

The porosity of SCG_0 and SCG-PEI-M_4 adsorbents were estimated by the BET adsorption isotherm analysis. The pore width, specific surface area and pore volume shown in Fig. 3 and Table 1 were calculated from the adsorption curve by the DFT method. SCG_0 sample shows a narrow distribution with pore size around 5 nm, whereas, SCG-PEI-M_4 has a wider pore distribution range, mainly between 5 and 10 nm, which belongs to mesopores. In this case, the size difference in two samples may result in a selectivity adsorption for dyes with different molar mass like CR and MB. The specific surface area and pore volume of SCG-PEI-M_4 increase by 4.666 m^2/g and 0.0031 cm^3/g because of the impregnation of PEI. This will improve the adsorption capacity of SCG-PEI-M_4 to dyes by the effect of pore filling.

3.1.3. FTIR and TG analysis

To check whether the PEI is successfully connected to SCG, the FTIR analysis was performed and the corresponding spectra of all adsorbents are shown in Fig. 4a. The wide peak at 3,330 cm^{-1} is generated by the overlap of O–H stretching and N–H stretching, demonstrating the existence of hydroxyl and amine groups in SCG. The intensive peak at 1,020 cm^{-1} is imputed to C–O–C stretching. The

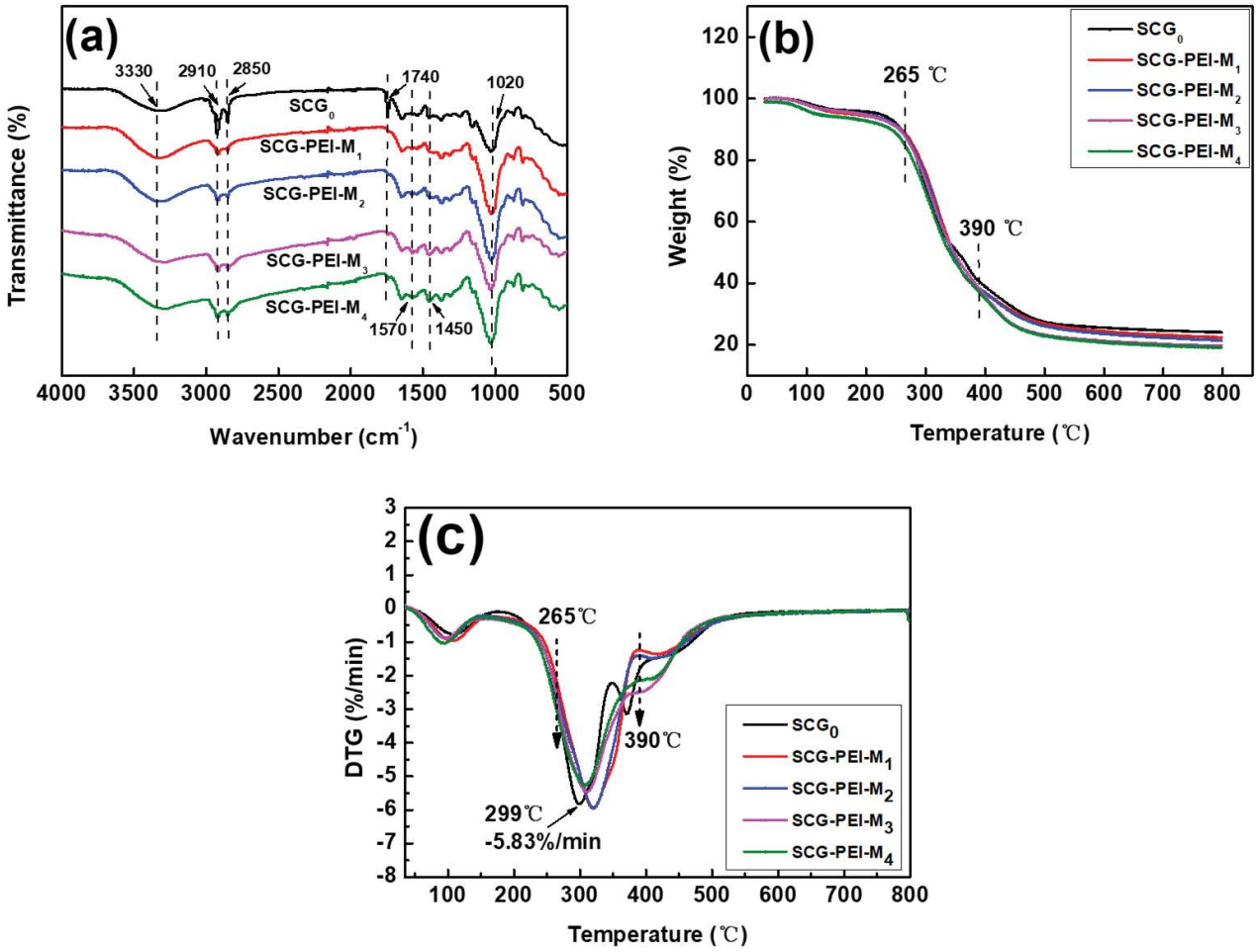

Fig. 4. Fourier-transform infrared spectra (a), thermogravimetric curves (b) and derivative thermogravimetry curves (c) of SCG_0 and SCG-PEI-M_x.

Table 1
Specific surface area and pore volume of SCG_0 and SCG-PEI-M_4

	SCG_0	SCG-PEI-M_4
Surface area (m^2/g)	13.670	18.336
Pore volume (cm^3/g)	0.0138	0.0169

characteristic peaks at 2,910 and 2,850 cm^{-1} [27] belong to C–H stretching which are derived from methylene groups in the cellulose component. The peak at 1,740 cm^{-1} [28] is attributed to the C=O stretching caused by carboxyl group in lignin. Compared with SCG_0, these peak values of SCG-PEI-M_x drop sharply because the carboxyl groups on SCG are partially replaced by the introduced PEI amino groups. Two strong peaks appeared at 1,570 and 1,450 cm^{-1} for SCG-PEI-M_x samples correspond to –NH_2 stretching and –NH bending, respectively. The fact that the SCG-PEI-M_4 sample has the highest characteristic peak intensity proves PEI has been introduced into SCG successfully.

Fig. 4b and c macroscopically depict the thermal degradation process of SCG_0 and SCG-PEI-M_x. In the range of 40°C–800°C, the degradation process of all samples consists of three stages. The main reason for the weight loss of samples in the first stage (40°C–265°C) is the evaporation of free water in the internal structure [29]. From 265°C to 390°C, the weight loss reached the highest, and as shown in Fig. 4c, the maximum weight loss rate was about –5.83%/min at 299°C, which is because of the breakdown of amino and hydroxyl groups in samples. When the temperature is higher than 390°C, the weight loss is mainly caused by the fracture and decomposition of the polymer skeleton. These results illustrate that the sample can withstand at about 265°C which is much higher than the adsorption temperature, making it has good thermal stability.

The weight loss percentage of SCG_0 and SCG-PEI-M_x over different temperature stages are shown in Table 2. The weight loss is less pronounced (about 3.87%–5.59%) in the first section, but reaches the highest in the second section. Here, the SCG_0 sample (57.54%) has the highest amount of degradation owing to the decomposition of hydroxyl groups in its structure, followed by the SCG-PEI-M_1 (56.05%) and SCG-PEI-M_2 (56.51%), which is attributed to the short chains attached on sample surface, as well as small amounts of amino groups in the long chain. SCG-PEI-M_3 (53.04%) and SCG-PEI-M_4 (54.07%) samples have the least amount

Table 2
Percentage of weight loss at each stage of SCG_0 and SCG-PEI-M_x

Sample	Weight loss in each stage (wt.%)		
	40°C–265°C	265°C–390°C	390°C–800°C
SCG_0	3.87	57.54	14.84
SCG-PEI-M_1	5.38	56.05	16.24
SCG-PEI-M_2	4.74	56.51	17.43
SCG-PEI-M_3	4.61	53.04	22.82
SCG-PEI-M_4	5.59	54.07	20.12

of degradation. As for the third stage, when the molecular weight of PEI contained in the samples becomes bigger, its degradation amount is basically larger.

3.1.4. XPS analysis

For estimating the existence of elements in SCG_0 and SCG-PEI-M_x, the full spectrum of all samples was analyzed using XPS, presented in Fig. 5a. The O1s element peak flatten out in SCG-PEI-M_x while the N1s and C1s element peaks enhance, which reveals that the –O group was translated to $–NH_2$ group with the action of amination, making the sample successfully aminated. To further confirm the above results, the elements in spectra were evaluated (Table 3). When the molecular weight of PEI raises (600–70,000), the content of N1s in SCG-PEI-M_x increases by 2.87%. A rapid growth (3.61%–5.75%) can be especially discovered when the molecular weight changes from 1800 to 10000.

The N element was analyzed to study the functional group changes of the SCG_0 and SCG-PEI-M_x adsorbents, revealed in Fig. 5b–f. Compare with SCG_0 sample, the peak areas of pyridine-N (N-6) (399.6 eV) and quaternary nitrogen (N-Q) (400.9 eV) in SCG-PEI-M_x samples gradually decrease, while the peak area of pyrrolic-N (N-5) (398.9 eV) increase markedly [30], which shows the existing mode of N element in SCG-PEI-M_x was mainly N-5. As shown in Table 4, with the increase of molecular weight of PEI in samples, the content of N-5 also increases, and reaches the maximum in SCG-PEI-M_4 sample (71.86%). These results indicate that N atom has been incorporated to carbon framework as desired and provide more active sites to enhance adsorption capacity.

3.2. Adsorption experiments

3.2.1. Effects of PEI molecular weight and dosage

For revealing the effects of PEI molecular weight (600, 1,800, 10,000, 70,000) on the dyes (CR and MB) adsorption behavior by SCG-PEI-M_x, the adsorption capacity and removal rate for CR and MB with different concentrations are exhibited in Fig. 6a and b (C_0 = 100–300 mg/L, 23°C, pH = 7). For all samples, a growth of adsorption ability with the concentration of CR can be viewed from Fig. 6a (histogram). This can be explained as the driving force for overcoming the mass transfer resistance between adsorbents and adsorbates increases with the augment of dye concentration, thus enhancing the attachment of CR. Furthermore, regardless of initial dye concentration, the adsorption ability of SCG_0 sample is quite weaker than that of SCG-PEI-M_x samples. As the molecular weight of PEI doped in SCG changes from 600, 1,800, 10,000 to 70,000, the adsorption amount for CR increases from 727, 751, 1,045 to 1,313 mg/g. The introduction of PEI provides more amino groups grafting on the SCG surface, and the high molecular weight of PEI increases the amounts of positive charges and improves the binding capacity of the adsorbent to anionic dyes. As can be seen from Fig. 6a (line chart) that when the CR concentration is 100 mg/L, the removal rate achieves the highest (87.1%), which is because the adsorbent with the same quality contains sufficient adsorption active sites and facilitates quick diffusion of dye molecular with low concentration. In summary, the selection of PEI with a molecular weight of 70,000 to modify SCG shows benefits to the adsorption of CR.

The changes of adsorption capacity (histogram) and removal rate (line chart) of SCG_0 for MB with initial concentration are presented in Fig. 6b. When the concentration of MB is the highest (300 mg/L), the adsorption capacity (814 mg/g) and removal rate (45.2%) of SCG_0 also reach the maximum. This phenomenon is attributed to high dye concentration provides more dye molecules for SCG_0 to adsorb. However, at the same concentration, the adsorption of SCG-PEI-M_x decreases in turn (783–637 mg/g), which is due to the positive charges in SCG-PEI-M_x reducing the binding ability of the cationic dye and the adsorbent, so that the adsorption capacity is lowed [31]. As the molecular weight of CR (M_w = 696.68 Da) is much higher than that of MB (M_w = 319.85 Da), SCG-PEI-M_4 with larger pore size is more propitious to adsorb dyes with larger molecular weight. The result is in good agreements with the BET analysis.

Different dosage of PEI (0, 1, 2, 3 g, M_w = 70000) was used to graft SCG_0 (1 g) to adsorb CR in the concentration range of 100–300 mg/L (23°C, pH = 7). It can be seen from Fig. 6c that samples grafting with PEI have better adsorption capacity when compared with SCG_0, proving the positive effect of PEI. Furthermore, adding 2 g (1,313 mg/g) PEI to SCG has the best impact, followed by 3 g (1,261 mg/g) and finally 1 g (1,188 mg/g), indicating that increase PEI dosage appropriately can introduce more amino groups, which can indeed improve the electrostatic binding ability of SCG and CR, leading a better adsorption capacity of CR. Excessive dosage will weaken the grafting effect. Therefore, the optimized mass ratio between SCG and PEI is 1:2, and the following experiment will be carried out under this condition.

3.2.2. Effects of pH

pH is a key element influencing the adsorption capability of SCG-PEI-M_4. The impact of the solution pH on the adsorption amount of CR by SCG-PEI-M_4 sample was estimated at the conditions of C_0 = 300 mg/L, 23°C, and pH = 4–10. Fig. 7a (black line) shows when the pH of CR ranges from 10 to 4, the adsorption capacity of SCG-PEI-M_4 increases from 1,049 to 1,496 mg/g. This tendency can be clearly viewed from the curve of absorbance vs. the pH of CR solution in Fig. 7b, the absorbance peak of the remaining dye liquid at 497 nm gradually dropped with the decrease of pH values, showing that more CR molecules has been

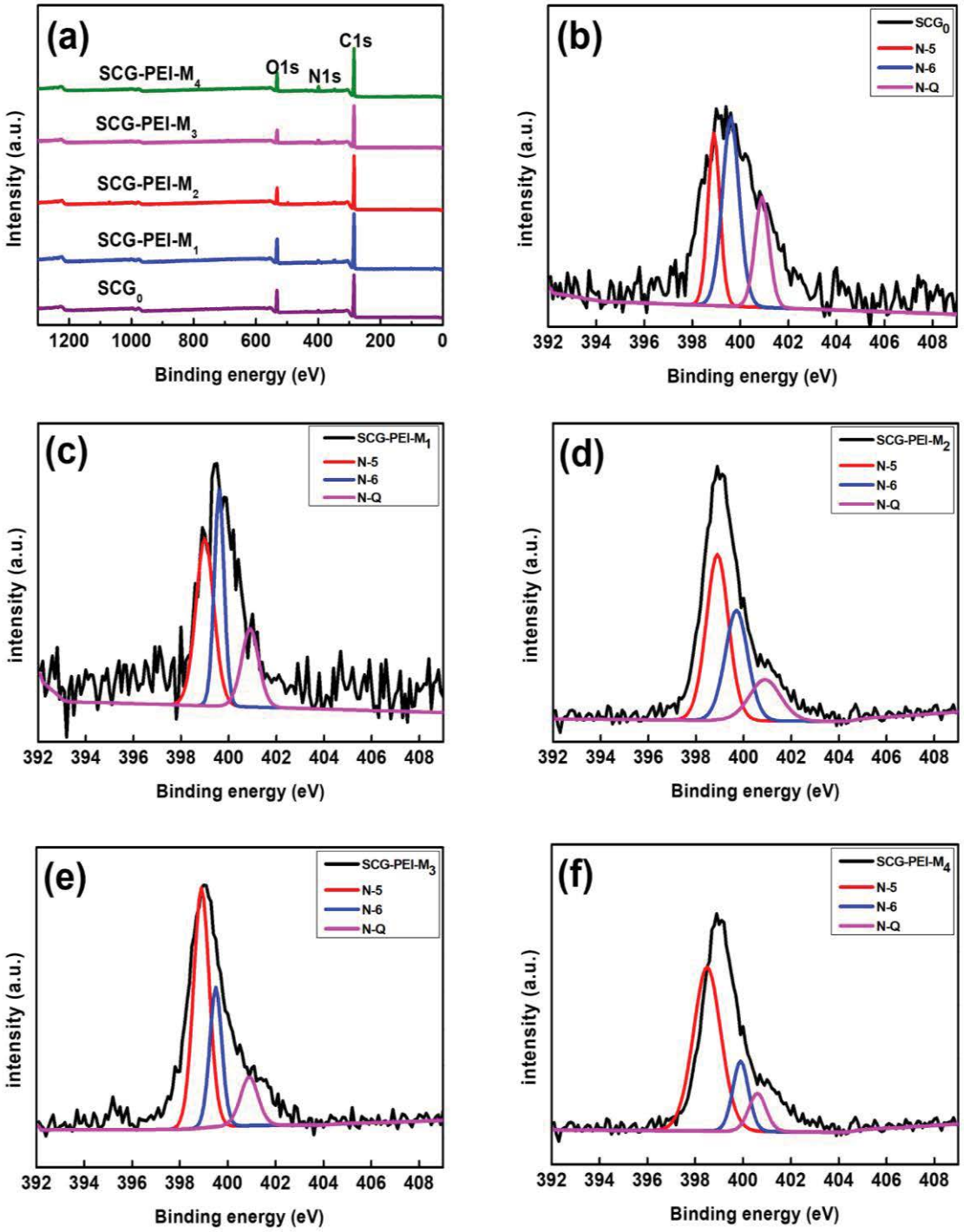

Fig. 5. X-ray photoelectron spectra of SCG_0 and SCG-PEI-M_x (a), N element in X-ray photoelectron spectra of SCG_0 (b) and SCG-PEI-M_x (c–f).

eliminated. For the higher the alkalinity of dye solutions, it has more hydroxide ion, the charge of the adsorbent surface switch from positive charge to negative charge. Moreover, hydroxide ions and dye molecules scramble for the active adsorption sites on adsorbent surface, so that reduce the adsorption of SCG-PEI-M_4 on CR. For the higher the acidity of CR, it contains more hydrogen ions and ammonia ions. This makes the surface groups of SCG-PEI-M_4 being protonated by positive charges, which can combine with more anionic CR by electrostatic attraction. To verify this, the surface charge of SCG-PEI-M_4 was tested and plotted with the pH of the solution in Fig. 7a (blue line), as the pH turns from 10 to 4, the charge of SCG-PEI-M_4 raises from –22.01 to 10.85 mV, demonstrating that the SCG-PEI-M_4 becomes

Table 3
Elements content of SCG_0 and SCG-PEI-M_x (%)

Sample	C1s	O1s	N1s
SCG-M_0	78.33	18.37	3.30
SCG-PEI-M_1	80.04	16.53	3.42
SCG-PEI-M_2	82.79	13.59	3.61
SCG-PEI-M_3	81.11	13.14	5.75
SCG-PEI-M_4	79.32	14.51	6.17

Table 4
Proportion of N1s functional groups in SCG_0 and SCG-PEI-M_x (%)

Sample	N-5	N-6	N-Q
SCG_0	30.02	47.00	22.99
SCG-PEI-M_1	46.44	32.73	20.83
SCG-PEI-M_2	49.34	33.39	17.27
SCG-PEI-M_3	59.56	26.84	13.60
SCG-PEI-M_4	71.86	17.60	10.54

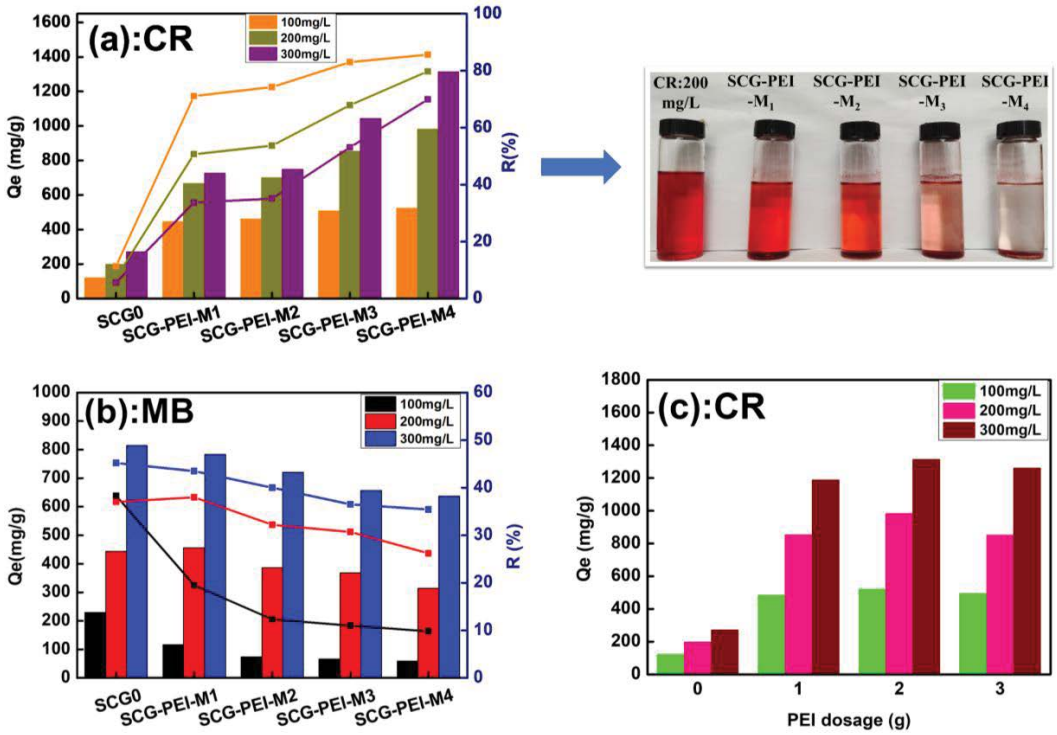

Fig. 6. Adsorption capacity (histogram) and removal rate (line chart) of SCG_0 and SCG-PEI-M_x at different initial concentrations of Congo red (a) and Methylene blue (b), changes of adsorption capacity of SCG-PEI-M_4 with different PEI dosage (c).

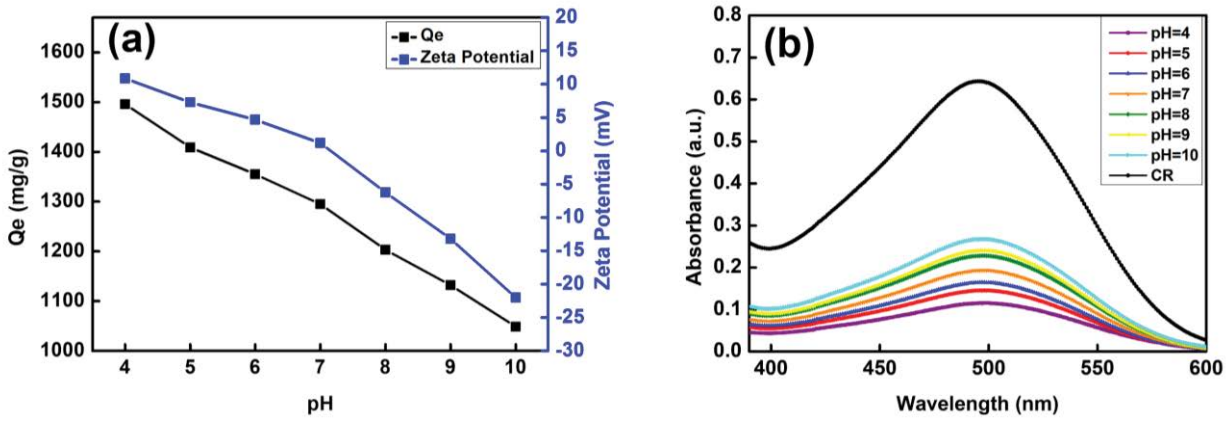

Fig. 7. Equilibrium adsorption capacity (black line in a) and zeta potential (blue line in a) of SCG-PEI-M_4 for Congo red in the range of pH = 4–10; UV absorbance of the solution after removal of Congo red (pH = 4–10) by SCG-PEI-M_4 (b).

more positive under acidic conditions, and has better adsorption capacity for CR at lower pH.

3.2.3. Adsorption kinetics studies

Fig. 8a shows the adsorption capacity of SCG-PEI-M_4 with different time at different concentrations of CR solution (23°C, pH = 7). The variation trends of these curves are identical, the adsorption capacity is dramatically increased in the first 10 h and nearly 90% CR was removed. With the delay of time, the adsorption capacity slowly elevates and eventually reaches equilibrium at the adsorption time of 48 h. The highest adsorption amount (1,313 mg/g) is achieved for CR with a concentration of 300 mg/L. It can be interpreted as in the initial stage, the adsorption process mainly depends on the strong electrostatic adsorption between the dye and the adsorbent. And the high concentration gradient between dye solutions and adsorbents surface causes a rapid diffusion of dye molecules from liquor towards the active sites in adsorbent, leading to a significant increase in adsorption capacity. After 10 h, the empty sites in adsorbent are continuously occupied by dye molecules and eventually saturated, the remaining dye can only fill in pores on the surface of the adsorbent. Due to the small pore size, the diffusion of dye molecules is hindered, which reduces the adsorption capacity and slows down the adsorption rate.

For studying the adsorption behaviors of SCG-PEI-M_4 under different concentration (100–300 mg/L) of CR, pseudo-first-order kinetic model [Eq. (4)], pseudo-second-order kinetic model [Eq. (5)] and Elovich model [Eq. (6)] were used to fit the adsorption process, respectively. Fig. 8b–g displayed that the Elovich dynamics model is well fit with the experimental data as comparing to pseudo-first-order and pseudo-second-order kinetic models. This result shows that adsorption behavior occurs on non-uniform solid surfaces. Detail information on kinetic parameters of CR removed by SCG-PEI-M_4 can be found in Table 5. In contrast to the pseudo-first-order kinetic model (0.8600–0.9478) and the pseudo-second-order kinetic model (0.9456–0.9829), the Elovich model (0.9074–0.9832) has a higher fitting parameter R^2. Consequently, the adsorption process of CR is more in line with Elovich kinetic model.

3.2.4. Isothermal study and adsorption thermodynamics

Fig. 9a exhibits the adsorption capacity of SCG-PEI-M_4 on CR under different concentrations (100–300 mg/L) and temperatures (298–328 K). The adsorption capacity of SCG-PEI-M_4 increases with adsorption temperature and CR concentration, and the maximum adsorption capacity reaches (1,610 mg/g) at the temperature of 328 K and CR concentration of 300 mg/L. The explanation is that the molecules of CR move faster at high temperature and thus gain more probability to enter the adsorbent sites and interact with amino groups. The adsorption behavior of SCG-PEI-M_4 on CR was judged from Langmuir model, Freundlich model and D-R model. Langmuir model implies that the solid surface is homogeneous and that only monomolecular layer adsorption occurs, while Freundlich model suggests that dyes are adsorbed in a multi-layered manner in a heterogeneous medium. Fig. 9b–e shows that both Langmuir and Freundlich models have a good fit for the adsorption of CR at 298–328 K. Analysis and comparison of the fitting parameters of three isotherm adsorption models using Eqs. (7)–(10) are displayed in Table 6. The fitting parameter R^2 value of Freundlich model (0.9970–0.9994) is bigger than that of the Langmuir model (0.9960–0.9987) and D-R model (0.8503–0.8939), representing the Freundlich model can successfully explicate the adsorption process of SCG-PEI-M_4. Hence, the adsorption of CR is part of multilayer adsorption on heterogeneous surface.

To study the internal energy change between adsorption process, the thermodynamic parameters obtained by Eqs. (11)–(13) are listed in Table 7 (C_0 = 100–300 mg/L, T = 298–328 K). At all concentrations of CR, both ΔH and ΔS are positive, suggesting the adsorption of CR by SCG-PEI-M_4 is an endothermic process. But ΔG is negative in any temperature, meaning the adsorption process is spontaneous [32]. Furthermore, the absolute value of ΔG becomes larger with the increment of temperature. In other words, the higher the temperature, the stronger the driving force of adsorption. Therefore, the adsorption of CR by SCG-PEI-M_4 occurs more easily and is the most effective at high temperature.

3.3. Adsorption mechanism for anionic dyes

The above experiments show that SCG-PEI-M_x samples have good adsorption performance on anionic CR. For a better understanding of the adsorption behavior, Fig. 10 shows the adsorption mechanism diagram of CR by the SCG-PEI-M_4 sample. And it mainly involves two effects: electrostatic force and pore filling. The former effect occurs mainly between the amino groups in SCG-PEI-M_4 and the sulfonic groups in CR, and the adsorption is independent of the amounts of amino groups in the sample. The latter effect is mostly related to the pore size which can selectively allow dye molecules with suitable size entering its pores.

The SCG-PEI-M_4 surface of before (Fig. 11a) and after adsorbing CR (Fig. 11b) were further imaged by SEM. Compared with SCG-PEI-M_4, the surface of the latter sample

Table 5
Parameters of three kinetic models at different Congo red concentrations

C_0 (mg/L)	Pseudo-first-order model			Pseudo-second-order model			Elovich model		
	R^2	Q_e (mg/g)	k_1 (h^{-1})	R^2	Q_e (mg/g)	k_2 (g/mg·h)	R^2	α (mg/g·h)	β (g/mg)
100	0.9478	470	1.08	0.9829	497	0.0030	0.9074	19,079	0.019
200	0.8855	907	0.27	0.9618	969	0.00047	0.9832	2,215	0.0070
300	0.8600	1,128	0.82	0.9456	1,225	0.00077	0.9781	9,724	0.0064

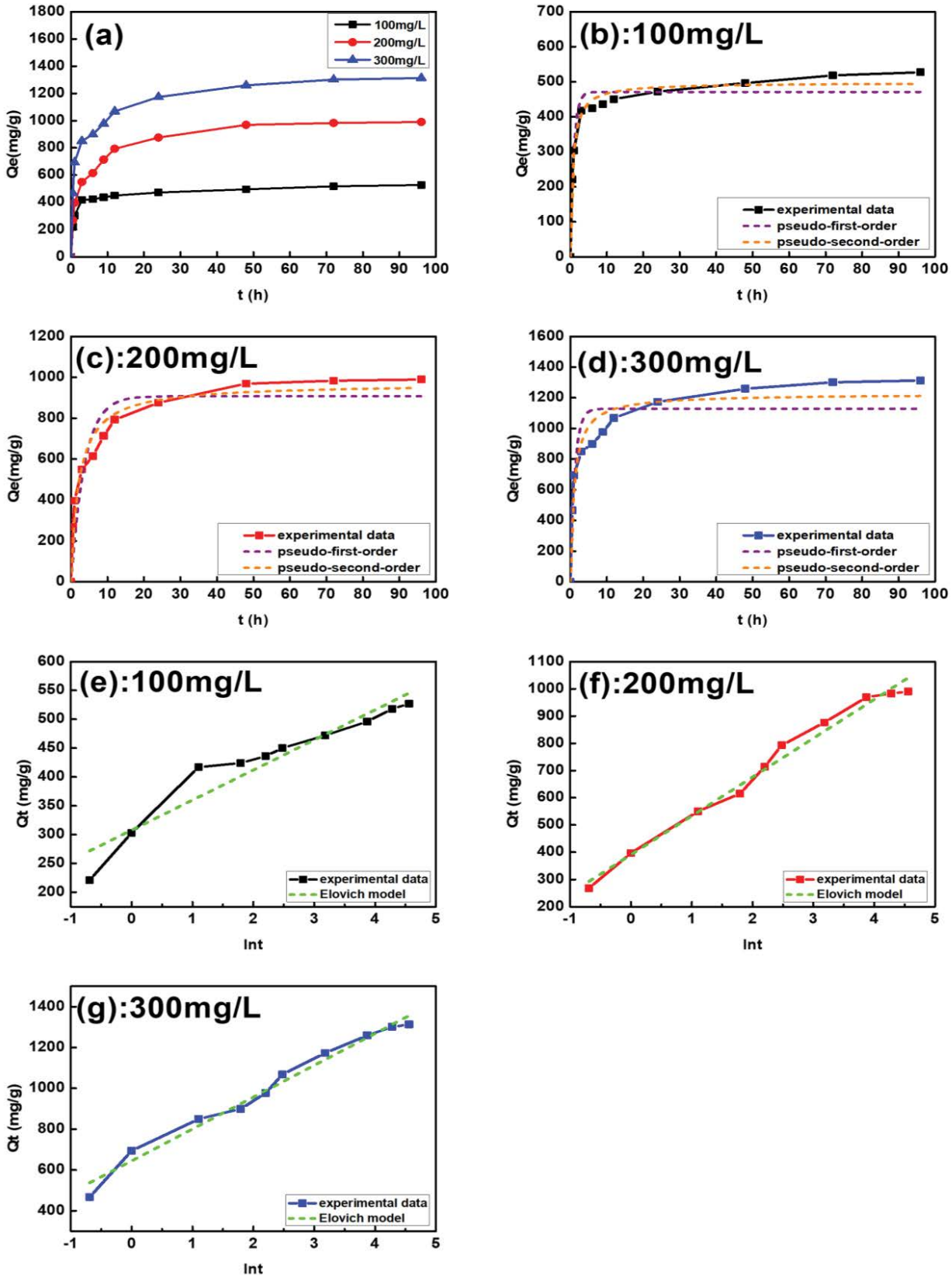

Fig. 8. Adsorption capacity of SCG-PEI-M_4 with different times at different concentrations of Congo red (100–300 mg/L) (a) and adsorption kinetic models of SCG-PEI-M_4 with different concentrations of Congo red (100–300 mg/L) (b–g).

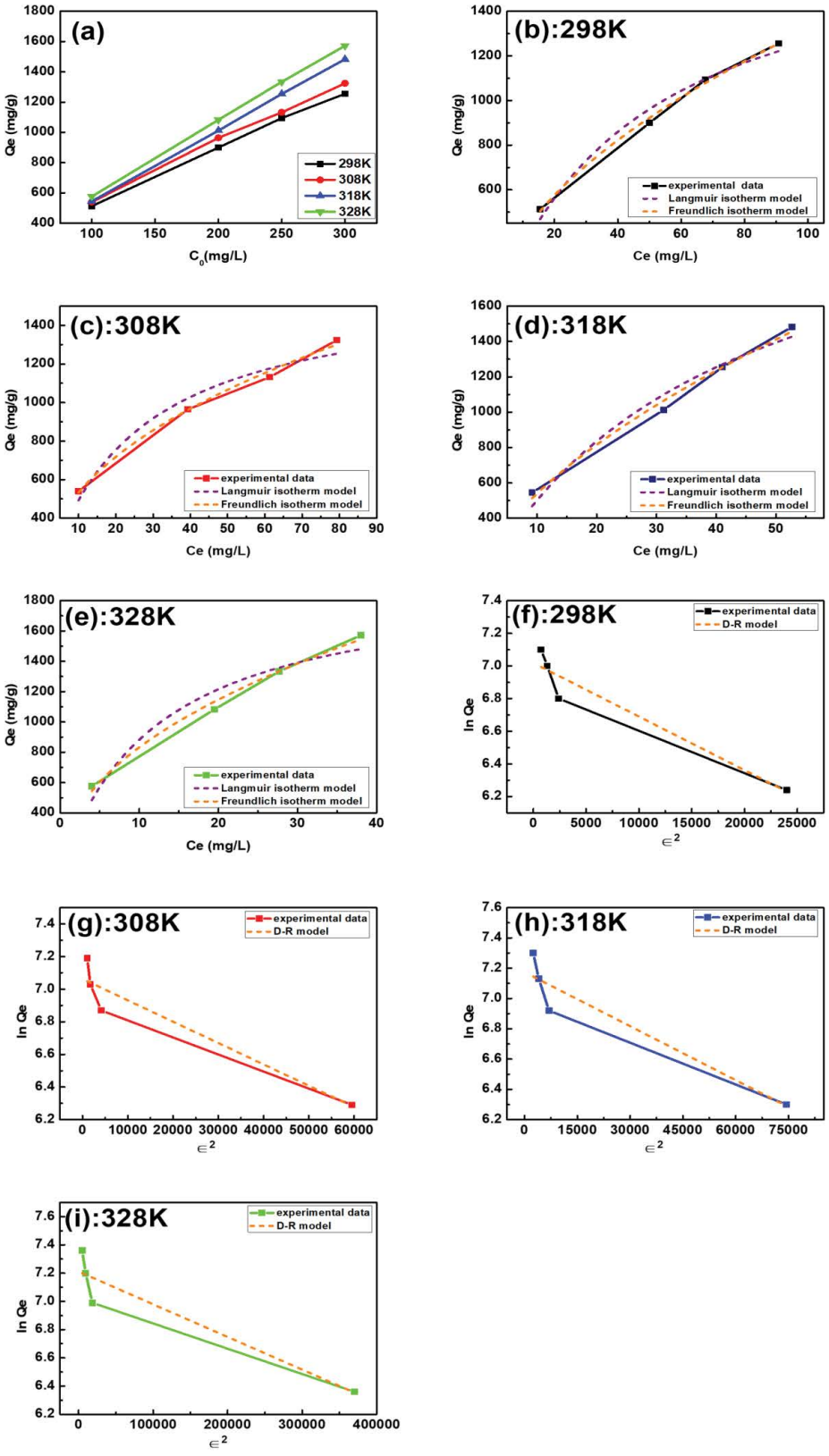

Fig. 9. Adsorption capacity of SCG-PEI-M_4 on Congo red under different concentrations (100–300 mg/L) and temperatures (298–328 K) (a); adsorption isothermal models of SCG-PEI-M_4 on Congo red with different concentrations at 298–328 K (b–i).

Table 6
Parameters of three isothermal adsorption models at 298–328 K

T (K)	Langmuir isotherm			Freundlich isotherm			Dubinin–Radushkevich isotherm		
	R^2	K_L (L/mg)	Q_m (mg/g)	R^2	K_F [(mg/g)(L/mg)$^{1/n}$]	n	R^2	K_{DR} (mol^2/J^2)	Q_m (mg/g)
298	0.9661	0.0223	1,824	0.9960	122.80	1.94	0.8939	3.28×10^{-5}	1,117
308	0.9439	0.0440	1,613	0.9927	197.78	2.32	0.8729	1.31×10^{-5}	1,167
318	0.9477	0.0248	2,518	0.9660	135.84	1.67	0.8596	1.19×10^{-5}	1,304
328	0.9120	0.0822	1,955	0.9881	286.27	2.16	0.8503	2.32×10^{-6}	1,354

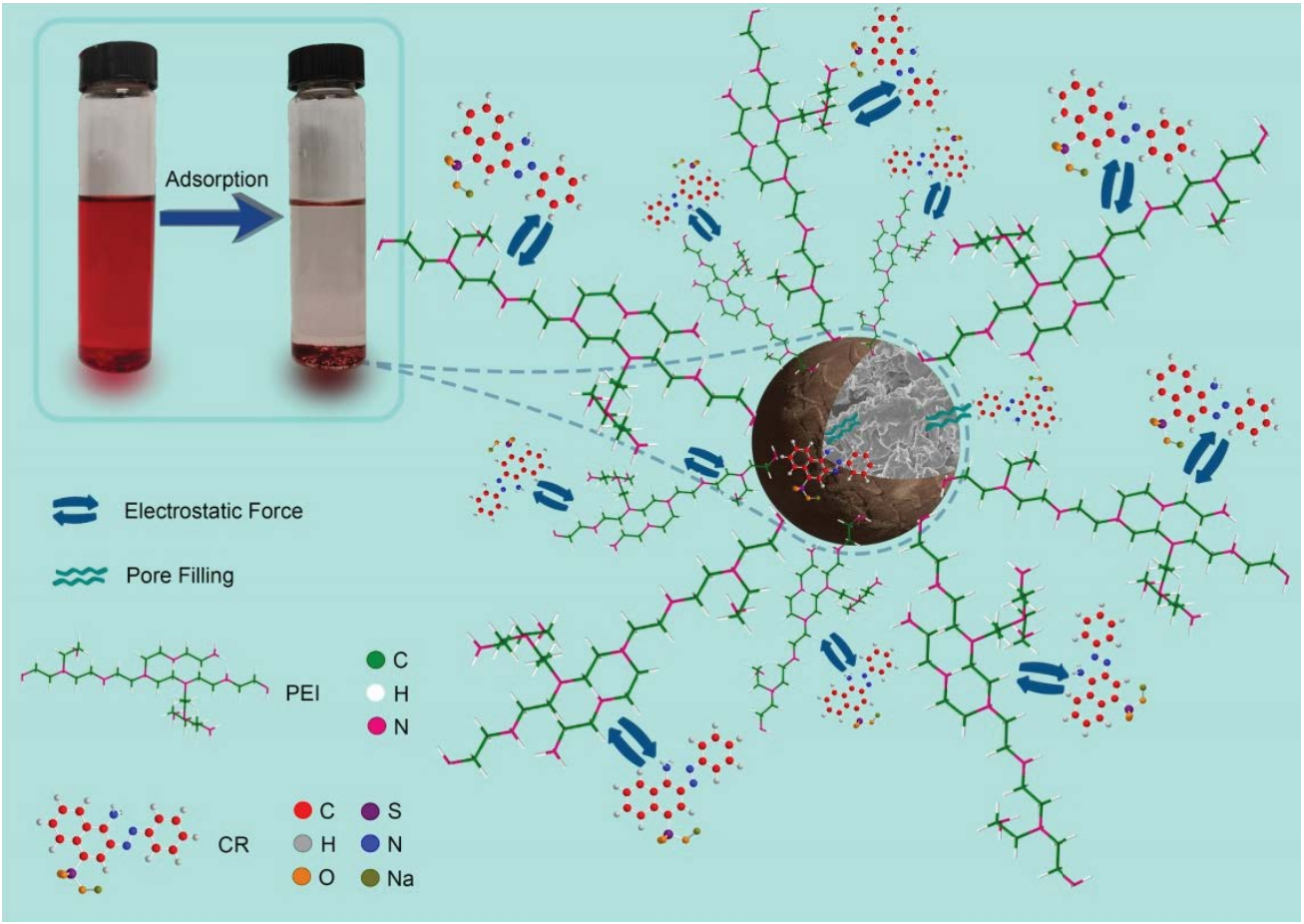

Fig. 10. Adsorption mechanism diagram of the SCG-PEI-M_4 for Congo red.

Table 7
Thermodynamic parameters of adsorption at different temperatures with different initial Congo red concentrations

C_0	ΔH	ΔS	ΔG (kJ/mol) at different temperature			
mg/L	kJ/mol	J/mol·K	298 K	308 K	318 K	328 K
100	2.77	22.95	–4.07	–4.30	–4.53	–4.76
200	5.05	29.43	–3.72	–4.01	–4.31	–4.60
250	5.44	30.43	–3.62	–3.93	–4.24	–4.54
300	7.50	36.83	–3.48	–3.84	–4.21	–4.58

seems more rougher and is covered with irregular clusters and small particles (indicated by red arrows). And the size ranges within micrometers. This verifies that the CR had been successfully adsorbed. Conclusively, the adsorbent prepared using PEI modified SCG has an excellent adsorption effect on CR.

3.4. Research progress of adsorbents

So far, a variety of environmentally friendly adsorbents have been used in the adsorption of dyes, including natural minerals, biosorbents and carbon nanomaterials. Their adsorption capacity for dyes is shown in Table 8. Among

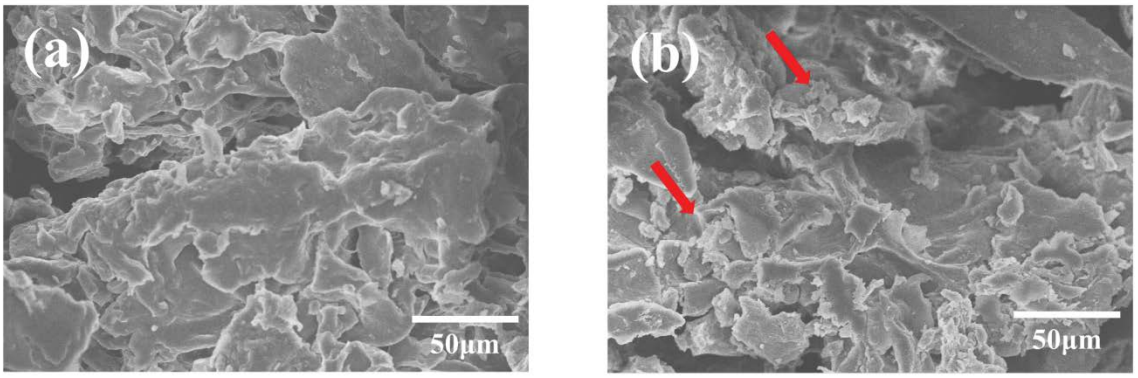

Fig. 11. Scanning electron microscopy images of SCG-PEI-M_4 before (a) and after (b) adsorbing Congo red.

Table 8
Adsorption capacity of different adsorbents for dyes

Adsorbents	Types of dyes	Q_m (mg/g)	Removal rate (%)	References
Montmorillonite-reduced graphene oxide aerogel	Methylene blue	450.9		[33]
Modified nanocellulose	Methylene blue		98%	[34]
Cellulose, clay and sodium alginate composites	Methylene blue		79%	[35]
Chitosan-based dual network composite hydrogel	Methylene blue	596.14		[36]
Modified natural polygorskite	Methylene blue	527.22		[37]
Fe_3O_4/Bi_2S_3 microspheres	Congo red	92.24		[38]
Polydopamine microspheres	Methylene blue	90.7		[39]

Table 9
Adsorption capacity of other SCG-based adsorbents for different dyes

Adsorbents	Types of dye	Q_m (mg/g)	References
Untreated coffee residues	Remazol Blue RN (RB)	179	[40]
	Basic Blue 3G (BB)	295	
CGAC	Nylosan Red N-2RBL(NR)	367	[16]
PEI-CW	RB5	77.52	[41]
	Congo red	34.36	
N-CGNM	Congo red	623.12	[30]
AC-ECRs	Acid Orange 7 (AO7)	1,222.5	[11]
SCG-GAC	AO7	665.9	[15]
	Methylene blue	986.8	
SCG-PEI-M_4	Congo red	1313	This work
SCG_0	Methylene blue	814	This work

them, there are few studies on the adsorption of CR and the selective adsorption of anionic and cationic dyes.

Table 9 further shows the adsorption amount of other SCG-based adsorbents for cationic and anionic dyes reported by previous studies. Compared with these adsorbents, the SCG-PEI-M_4 sample prepared in this paper has high adsorption capacity for CR leading to high applicability.

4. Conclusion

In this paper, SCG-PEI-M_4 and SCG_0 samples were evaluated as potential adsorbents in removing CR and MB with the maximum adsorption capacities of 1,313 and 814 mg/g, respectively. In terms of T = 328 K, C_0 = 300 mg/L and pH = 4, the adsorption capacity of SCG-PEI-M_4 for CR achieved the highest. The adsorption process is complied with Elovich kinetic model and Freundlich adsorption isotherm model, which means the adsorption of CR on the surface of the SCG-PEI-M_4 belongs to multi-layer adsorption. The adsorption effect of SCG-PEI-M_4 on CR is obviously better than that of MB, because PEI provides a lot of amino groups and introduces a positive charge to the sample surface, which improves the binding ability between the sample and anionic dyes. The adsorption mechanism further

indicates that the binding force between SCG-PEI-M_4 and CR is dominated by electrostatic force and pore filling.

Acknowledgement

This work was supported by the National Natural Science Foundation of China (Grant No. 51378350) and the Nature Science Foundation of Tianjin City (Grant No. 17JCTPJC47000).

References

[1] E. Pagalan Jr., M. Sebron, S. Gomez, S.J. Salva, R. Ampusta, A.J. Macarayo, C. Joyno, A. Ido, R. Arazo, Activated carbon from spent coffee grounds as an adsorbent for treatment of water contaminated by aniline yellow dye, Ind. Crops Prod., 145 (2020) 111953, doi: 10.1016/j.indcrop.2019.111953.
[2] M. Novotna, P. Knotek, T. Hanzlicek, P. Kutalek, I. Perna, K. Melanova, E. Cernoskova, K. Kopecka, TiO_2 modified geopolymers for the photocatalytic dye decomposition, Crystals, 11 (2021) 1511, doi: 10.3390/cryst11121511.
[3] D.C. Roy, S.K. Biswas, A.K. Saha, B. Sikdar, M. Rahman, A.K. Roy, Z.H. Prodhan, S.-S. Tang, Biodegradation of Crystal violet dye by bacteria isolated from textile industry effluents, PeerJ, 6 (2018) e5015, doi: 10.7717/peerj.5015.
[4] M. Ensafi Avval, P.N. Moghadam, M.M. Baradarani, Synthesis of a new nanocomposite based-on graphene-oxide for selective removal of Pb^{2+} ions from aqueous solutions, Polym. Compos., 40 (2018) 730–737.
[5] H. Ahmad, M. Zahid, Z.A. Rehan, A. Rashid, S. Akram, M.M.H. Aljohani, S.K. Mustafa, T. Khalid, N.R. Abdelsalam, R.Y. Ghareeb, M.S. AL-Harbi, Preparation of polyvinylidene fluoride nano-filtration membranes modified with functionalized graphene oxide for textile dye removal, Membranes, 12 (2022) 224, doi: 10.3390/membranes12020224.
[6] N.A.M. Zainuddin, N. Azmi, S.W. Puasa, S.R.M. Yatim, Response surface methodology and kinetic study for removal of colour and chemical oxygen demand from coffee wastewater by using spent coffee grounds, Desal. Water Treat., 257 (2022) 228–242.
[7] M. El Khomri, N. El Messaoudi, A. Dbik, S. Bentahar, A. Lacherai, N. Faska, A. Jada, Regeneration of argan nutshell and almond shell using HNO_3 for their reusability to remove cationic dye from aqueous solution, Chem. Eng. Commun., 209 (2022) 1304–1315.
[8] S.N. Jain, S.R. Tamboli, D.S. Sutar, S.R. Jadhav, J.V. Marathe, A.A. Shaikh, A.A. Prajapati, Batch and continuous studies for adsorption of anionic dye onto waste tea residue: kinetic, equilibrium, breakthrough and reusability studies, J. Cleaner Prod., 252 (2020) 119778, doi: 10.1016/j.jclepro.2019.119778.
[9] J.Z. Ma, L.Y. Hou, P. Li, S.M. Zhang, X.Y. Zheng, Modified fruit pericarp as an effective biosorbent for removing azo dye from aqueous solution: study of adsorption properties and mechanisms, Environ. Eng. Res., 27 (2022) 200634, doi: 10.4491/eer.2020.634.
[10] H. Singh, S. Choden, Comparison of adsorption behaviour and kinetic modeling of bio-waste materials using basic dye as adsorbate, Indian J. Chem. Technol., 21 (2014) 359–367.
[11] K.-W. Jung, B.H. Choi, M.-J. Hwang, J.-W. Choi, S.-H. Lee, J.-S. Chang, K.-H. Ahn, Adsorptive removal of anionic azo dye from aqueous solution using activated carbon derived from extracted coffee residues, J. Cleaner Prod., 166 (2017) 360–368.
[12] B. Sukhbaatar, B. Yoo, J.-H. Lim, Metal-free high-adsorption-capacity adsorbent derived from spent coffee grounds for Methylene blue, RSC Adv., 11 (2021) 5118–5127.
[13] A.S. Franca, L.S. Oliveira, M.E. Ferreira, Kinetics and equilibrium studies of Methylene blue adsorption by spent coffee grounds, Desalination, 249 (2009) 267–272.
[14] C.-H. Chiang, J. Chen, J.-H. Lin, Preparation of pore-size tunable activated carbon derived from waste coffee grounds for high adsorption capacities of organic dyes, J. Environ. Chem. Eng., 8 (2020) 103929, doi: 10.1016/j.jece.2020.103929.
[15] K.-W. Jung, B.H. Choi, M.-J. Hwang, T.-U. Jeong, K.-H. Ahn, Fabrication of granular activated carbons derived from spent coffee grounds by entrapment in calcium alginate beads for adsorption of acid orange 7 and Methylene blue, Bioresour. Technol., 219 (2016) 185–195.
[16] A. Reffas, V. Bernardet, B. David, L. Reinert, M.B. Lehocine, M. Dubois, N. Batisse, L. Duclaux, Carbons prepared from coffee grounds by H_3PO_4 activation: characterization and adsorption of Methylene blue and Nylosan Red N-2RBL, J. Hazard. Mater., 175 (2010) 779–788.
[17] R. Bushra, S. Mohamad, Y. Alias, Y. Jin, M. Ahmad, Current approaches and methodologies to explore the perceptive adsorption mechanism of dyes on low-cost agricultural waste: a review, Microporous Mesoporous Mater., 319 (2021) 111040, doi: 10.1016/j.micromeso.2021.111040.
[18] Q. Chen, Y. Zhao, Q. Xie, C. Liang, Z. Zong, Polyethyleneimine grafted starch nanocrystals as a novel biosorbent for efficient removal of methyl blue dye, Carbohydr. Polym., 273 (2021) 118579, doi: 10.1016/j.carbpol.2021.118579.
[19] L. Hao, P. Wang, S. Valiyaveettil, Successive extraction of As(V), Cu(II) and P(V) ions from water using spent coffee powder as renewable bioadsorbents, Sci. Rep., 7 (2017) 42881, doi: 10.1038/srep42881.
[20] Z. Chen, J. Zeng, Z.B. Zhang, Z.J. Zhang, S. Ma, C.M. Tang, J.Q. Xu, Preparation and application of polyethyleneimine-modified corncob magnetic gel for removal of Pb(II) and Cu(II) ions from aqueous solution, RSC Adv., 12 (2022) 1950–1960.
[21] S. Wong, H.H. Tumari, N. Ngadi, N.B. Mohamed, O. Hassan, R. Mat, N.A. Saidina Amin, Adsorption of anionic dyes on spent tea leaves modified with polyethyleneimine (PEI-STL), J. Cleaner Prod., 206 (2019) 394–406.
[22] F. Taleb, M. Ammar, M.B. Mosbah, R.B. Salem, Y. Moussaoui, Chemical modification of lignin derived from spent coffee grounds for Methylene blue adsorption, Sci. Rep., 10 (2020) 11048, doi: 10.1038/s41598-020-68047-6.
[23] M.S. Akindolie, H.J. Choi, Surface modification of spent coffee grounds using phosphoric acid for enhancement of Methylene blue adsorption from aqueous solution, Water Sci. Technol., 85 (2022) 1218–1234.
[24] M. Kumar, H.S. Dosanjh, H. Singh, Biopolymer modified transition metal spinel ferrites for removal of fluoride ions from water, Environ. Nanotechnol. Monit. Manage., 12 (2019) 100237, doi: 10.1016/j.enmm.2019.100237.
[25] V.K. Rattan, H. Singh, Adsorption of nickel from aqueous solutions using low cost biowaste adsorbents, Water Qual. Res. J., 46 (2011) 239–249.
[26] S. Abuzerr, M. Darwish, A.H. Mahvi, Simultaneous removal of cationic Methylene blue and anionic Reactive Red 198 dyes using magnetic activated carbon nanoparticles: equilibrium, and kinetics analysis, Water Sci. Technol., 2 (2018) 534–545.
[27] S. Wong, Y. Lim, N. Ngadi, R. Mat, O. Hassan, I.M. Inuwa, N.B. Mohamed, J.H. Low, Removal of acetaminophen by activated carbon synthesized from spent tea leaves: equilibrium, kinetics and thermodynamics studies, Powder Technol., 338 (2018) 878–886.
[28] R. Lafi, A. ben Fradj, A. Hafiane, B.H. Hameed, Coffee waste as potential adsorbent for the removal of basic dyes from aqueous solution, Korean J. Chem. Eng., 31 (2014) 2198–2206.
[29] G. Wang, G. Li, Y. Huan, C. Hao, W. Chen, Acrylic acid functionalized graphene oxide: high-efficient removal of cationic dyes from wastewater and exploration on adsorption mechanism, Chemosphere, 261 (2020) 127736, doi: 10.1016/j.chemosphere.2020.127736.
[30] Z. Dai, P.-G. Ren, H. Zhang, X. Gao, Y.-L. Jin, Nitrogen-doped and hierarchically porous carbon derived from spent coffee ground for efficient adsorption of organic dyes, Carbon Lett., 31 (2021) 1249–1260.
[31] X. Huang, B.H. Li, S.B. Wang, X.Y. Yue, Z.G. Yu, X.J. Deng, J.M. Ma, Facile *in-situ* synthesis of PEI-Pt modified bacterial cellulose bio-adsorbent and its distinctly selective adsorption

of anionic dyes, Colloids Surf., A, 586 (2020) 124163, doi: 10.1016/j.colsurfa.2019.124163.
[32] C.Q. Hao, G.F. Li, G.L. Wang, W. Chen, S.S. Wang, Preparation of acrylic acid modified alkalized MXene adsorbent and study on its dye adsorption performance, Colloids Surf., A, 632 (2022) 127730, doi: 10.1016/j.colsurfa.2021.127730.
[33] S. Zhou, J. Yin, Q. Ma, B. Baihetiyaer, J. Sun, Y. Zhang, Y. Jiang, J. Wang, X. Yin, Montmorillonite-reduced graphene oxide composite aerogel (M−rGO): a green adsorbent for the dynamic removal of cadmium and Methylene blue from wastewater, Sep. Purif. Technol., 296 (2022) 121416, doi: 10.1016/j.seppur.2022.121416.
[34] T. Shahnaz, D. Bedadeep, S. Narayanasamy, Investigation of the adsorptive removal of Methylene blue using modified nanocellulose, Int. J. Biol. Macromol., 200 (2022) 162–171.
[35] A. Kausar, S.U. Rehman, F. Khalid, A. Bonilla-Petriciolet, D.I. Mendoza-Castillo, H.N. Bhatti, S.M. Ibrahim, M. Iqbal, Cellulose, clay and sodium alginate composites for the removal of Methylene blue dye: experimental and DFT studies, Int. J. Biol. Macromol., 209 (2022) 576–585.
[36] X. Wan, Z. Rong, K. Zhu, Y. Wu, Chitosan-based dual network composite hydrogel for efficient adsorption of Methylene blue dye, Int. J. Biol. Macromol., 222 (2022) 725–735.
[37] W.B. Wang, G.Y. Tian, Z.F. Zhang, A.Q. Wang, A simple hydrothermal approach to modify palygorskite for high-efficient adsorption of Methylene blue and Cu(II) ions, Chem. Eng. J., 265 (2015) 228–238.
[38] H.Y. Zhu, R. Jiang, J.B. Li, Y.Q. Fu, S.T. Jiang, J. Yao, Magnetically recyclable Fe_3O_4/Bi_2S_3 microspheres for effective removal of Congo red dye by simultaneous adsorption and photocatalytic regeneration, Sep. Purif. Technol., 179 (2017) 184–193.
[39] J.W. Fu, Z.H. Chen, M.H. Wang, S.J. Liu, J.H. Zhang, J.N. Zhang, R.P. Han, Q. Xu, Adsorption of Methylene blue by a high-efficiency adsorbent (polydopamine microspheres): kinetics, isotherm, thermodynamics and mechanism analysis, Chem. Eng. J., 259 (2015) 53–61.
[40] G.Z. Kyzas, N.K. Lazaridis, A.C. Mitropoulos, Removal of dyes from aqueous solutions with untreated coffee residues as potential low-cost adsorbents: equilibrium, reuse and thermodynamic approach, Chem. Eng. J., 189 (2012) 148–159.
[41] S. Wong, N.A. Ghafar, N. Ngadi, F.A. Razmi, I.M. Inuwa, R. Mat, N.A.S. Amin, Effective removal of anionic textile dyes using adsorbent synthesized from coffee waste, Sci. Rep., 10 (2020) 2928, doi: 10.1038/s41598-020-60021-6.